8-Quinoline based ligands and their metallic derivatives: A structural and statistical investigation of quinoline π–π stacking interactions†

Radu F. Semeniuc,*[a] Thomas J. Reamer[a] and Mark D. Smith[b]

Received (in Victoria, Australia) 8th October 2009, Accepted 24th November 2009
First published as an Advance Article on the web 26th January 2010
DOI: 10.1039/b9nj00547a

The new ligand 8-sulfonyl-(1-pyrazolyl)-quinoline, (C_9H_6N–SO_2-pz, **L**), which combines two different aromatic rings with donor properties in one molecule (a quinoline moiety functionalized with a pyrazolyl ring through a sulfonyl bridge) has been synthesized and characterized in both solution and solid state. **L** reacts with AgO_3SCF_3 (AgOTf) and $AgBF_4$ to form discrete compounds (C_9H_6N–SO_2-pz)$_2AgO_3SCF_3$ (**1**) and (C_9H_6N–SO_2-pz)$_2AgBF_4$ (**2**). Supramolecular associations were observed in all cases, based on a similar association algorithm, involving the π–π stacking of the quinoline tectons. The presence of the pyrazolyl ring in an appropriate position with respect to the quinoline moiety makes possible the occurrence of additional C–H···π interactions between the aromatic rings. These interactions generate dimers in all cases, and in two cases (**L** and compound **1**) the dimers undergo further self-assembly into higher dimension architectures, based either on π–π stacking interactions alone (**L**) or on combined π–π stacking/C–H···π interactions of the quinoline and pyrazolyl groups (**1**). A geometrical and statistical analysis has also been performed on π–π stacking in metal complexes of quinoline based ligands, by carrying out a Cambridge Structural Database search. The search showed that this interaction is relatively common for metal complexes of functionalized quinoline based ligands and occurs in 69% of all cases. At its simplest level, such an interaction produces discrete dimeric species. Higher dimensionality networks are obtained either by the extension of the π–π stacking interactions in one or more dimensions, or by bringing into play other supramolecular synthons, such as hydrogen bonding or C–H···π interactions.

Introduction

Crystal engineering is the rational design of functional molecular solids[1] and is defined as "the modeling, synthesis and evaluation of the properties of crystalline materials".[1a] This area of research is of both fundamental and practical interest to solid-state and structural chemists, and also important to other fields dealing with organized phases and assemblies.[1b,c] The goal of crystal engineering is the assembly of functionalized building blocks into an architecture that would show combined (supramolecular) properties based on the individual properties of the building blocks.[1f] A prerequisite in reaching this goal is a complete understanding and control of intra- and intermolecular forces and of the supramolecular self-assembly process. Advances in this field are based on finding reliable supramolecular synthons[1n,o] that can be used to formulate an algorithmic approach to the design of solids. Hydrogen bonding is a widely used tool in crystal engineering because its directionality and robustness makes its associative protocol possible to be transferred from one system to another.[2] Using graph-set descriptors, various motifs of hydrogen bonding were documented by Allan *et al.*, after a systematic analysis of the probabilities of formation of hydrogen-bonded ring motifs in organic crystal structures found in the Cambridge Structural Database (CSD).[3] For the 75 hydrogen bonding motifs revealed, they presented both the geometrical descriptions of the interactions and their probability of formation, thus providing insights into the relative robustness of known and potential supramolecular synthons.

Another supramolecular motif was introduced by Ian Dance and first called 'phenyl embrace'.[4] It consists of a concerted set of interactions between phenyl groups through a combination of offset face-to-face π–π stacking and C–H···π interactions. They are attractive in their nature, having energies up to 16 kcal/mol.[5] This intermolecular arrangement was first observed in phenylated moieties of the formula $[PPh_4]^+$ and then extended to other aromatic systems such as 2,2′-bipyridine, terpyridine, and 1,10-phenanthroline, thus the generic term was changed to "aryl embrace".[6] Later it was observed that similar interactions occur in systems where the aromatic moieties were connected through flexible spacers.[7] Studies on the probability of formation of this supramolecular motif were performed on chemical species of the general formula—EPh_3 (where E = any tetrahedral atom) and a wide range of values were found, from 0% to 62%—depending on the central atom.[8]

Later it was shown that smaller rings such as pyrazole can also be involved in similar embraces, either with itself or in

[a] *Department of Chemistry, Eastern Illinois University, Charleston, IL 61920, USA. E-mail: rsemeniuc@eiu.edu; Fax: +1 217 581 6613; Tel: +1 217 581 5422*
[b] *Department of Chemistry and Biochemistry, University of South Carolina, Columbia, SC 29208, USA*

† Electronic supplementary information (ESI) available: Crystallographic data in CIF format and figures of selected examples from literature. CCDC reference numbers 750912–750914. For ESI and crystallographic data in CIF or other electronic format see DOI: 10.1039/b9nj00547a

combination with larger, pyridine based aromatic systems, where the building blocks were associated as well by cooperative π–π and C–H···π interactions.[9] It was demonstrated that regardless of which rings were involved in the π–π stacking component of the embrace, they were always of the same type, that is they always had the same number of atoms within the ring.

The common denominator of all these embraces is a π–π stacking interaction of (functionalized) aromatic hydrocarbons, that are further supported by additional C–H···π interactions. In contrast to hydrogen bonding, π–π stacking has a less predictable directional associative protocol, due to the fact that variable orientations of the stacked moieties often occur in order to maximize the electrostatic attraction between the σ framework and the π electron density of the stacked groups.[10] Although association of several π species in solution was substantiated in some cases, there is still much to learn about their solution structure and their relative orientation.[11]

Still, much work and effort is needed in order to lay a foundation for a "grand unified supramolecular theory" with practical applications in the field of crystal engineering, especially because different interactions can appear between the same functional groups, thus leading to the appearance of polymorphs or pseudo-polymorphs, so that it is difficult to anticipate the resulting crystal structure without also taking into account other factors related to the crystallization step of a given set of chemical species that incorporate the same synthons. To overcome these drawbacks, three distinct, but related research directions should be pursued: (a) the study of *all* intermolecular interactions, especially their interdependence within the same system;[12] (b) establishing the relationship between the molecular synthons and crystal packing generated by them;[13] and (c) improving the crystal properties, based on a better control of the synthons.[14]

Several such studies are based on metal containing building blocks. The metal ions play two essential functions in the self-assembly process of the components into the target (discrete or infinite) architectures: a structural task by directing and supporting the solid-state architecture and a functional role by bringing the desired properties into the final network.[15] The silver(I) ion has been extensively employed in the assembly of a large number of both discrete compounds and coordination polymers.[16] The flexibility of its coordination sphere can produce sophisticated coordination architectures, but the structures are less predictable than with other metals. It is this flexibility that affords an opportunity to investigate how the self-assembly process is influenced by modifications of the ligand denticity, the ligand-to-metal ratio, the counterions, and non-covalent interactions.[10,16,17] Therefore, insight into the self-assembly process can be obtained by carrying out systematic studies using a series of similar complexes assembled from a specific ligand and imposing subtle alterations in the environment, for example changing the anions, the solvent, and/or the ligand-to-metal ratio.

Reported here are results obtained by preparing a new ligand that combines two different aromatic rings with Lewis donor properties in one molecule (a quinoline moiety and a pyrazolyl ring linked through a sulfonyl bridge), which has been characterized in both solution and solid state. Also reported are the reactions of this ligand with silver(I) salts to form discrete compounds that have different supramolecular structures, although based on a similar association algorithm involving concerted π–π stacking/C–H···π interactions of the quinoline and pyrazolyl groups. A geometrical and statistical analysis has also been performed on π–π stacking in metal complexes of substituted quinoline based ligands, by carrying out a Cambridge Structural Database search, which showed that this interaction is relatively common for metal complexes containing the quinoline moiety.

Experimental

General considerations

All operations were carried out under a nitrogen atmosphere using standard Schlenk techniques and a MBraun LabStar dry-box. Solvents were dried by conventional methods and distilled under a dry N_2 atmosphere immediately prior to use. Elemental analyses were performed by Robertson Microlit Laboratories. NMR spectra were recorded by using a 400 MHz Bruker Avance FT-NMR Spectrometer. All reagents are commercially available (Sigma-Aldrich) and were used without further purification.

Syntheses

8-Sulfonyl-(1-pyrazolyl)-quinoline, C_9H_6N–SO_2-pz (L). Pyrazole (0.680 g, 9.98 mmol) was dissolved in dry THF (50 mL) and added dropwise to a suspension of NaH (0.24 g, 10 mmol) in dry THF (100 mL) under an inert atmosphere. The mixture was stirred at room temperature for 1 h. To this solution was added dropwise a solution of 8-quinoline-sulfonyl chloride (2.276 g, 9.99 mmol) in dry THF (150 mL) and the resulting mixture was stirred at room temperature overnight. The resulting NaCl was filtered off and the THF removed under reduced pressure, to afford the desired compound as a white powder (2.437 g, 93.9%). ^{1}H-NMR (400 MHz, acetone-d_6): δ: 8.96 (dd, J_1 = 1.68, J_2 = 3.88, 1H, *quinoline*); 8.70 (dd, J_1 = 0.84, J_2 = 2.64, 1H, 5-*pz*); 8.64 (dd, J_1 = 1.48, J_2 = 7.4, 1H, *quinoline*); 8.51 (dd, J_1 = 1.8, J_2 = 8.36, 1H, *quinoline*); 8.42 (dd, J_1 = 1.32, J_2 = 8.2, 1H, *quinoline*); 7.89 (t, J = 7.76, 1H, *quinoline*); 7.67 (m, 1H, *quinoline*); 7.64 (d, J = 1.0, 1H, 3-*pz*); 6.48 (dd, J_1 = 1.48, J_2 = 2.8, 1H, 4-*pz*); Anal. Calcd. for $C_{12}H_9N_3O_2S$: C, 55.59; H, 3.50; N, 16.21. Found C, 55.27; H, 3.31, N, 16.46.

(C_9H_6N–SO_2-pz)$_2$$AgO_3SCF_3$ (1). A solution containing **L** (0.518 g, 1.99 mmol) in dry THF (50 mL) was added dropwise to a solution of AgO_3SCF_3 (0.257 g, 1.0 mmol) in dry THF (25 mL). Upon stirring for 12 h a white precipitate formed. The solvent was filtered off to leave a white solid (0.692 g, 89.2%) identified as L_2AgOTf (**1**); ^{1}H-NMR (400 MHz, acetone-d_6): δ: 9.13 (dd, J_1 = 1.68, J_2 = 6.0, 1H, *quinoline*); 8.80 (dd, J_1 = 1.32, J_2 = 7.48, 1H, *quinoline*); 8.75 (d, J = 2.84, 1H, 5-*pz*); 8.64 (dd, J_1 = 1.68, J_2 = 8.36, 1H, *quinoline*); 8.51 (dd, J_1 = 1.24, J_2 = 8.24, 1H, *quinoline*); 7.92 (m, 2H, *quinoline* + 3-*pz*); 7.76 (m, 1H, *quinoline*); 6.67 (dd, J_1 = 1.68, J_2 = 2.72, 1H, 4-*pz*); Anal. Calcd. for $C_{25}H_{18}AgF_3N_6O_7S_3$: C, 38.72; H, 2.34; N, 10.84. Found C, 39.04; H, 2.65; N, 11.07.

(C_9H_6N–SO_2-pz)$_2AgBF_4$ (2). This compound was prepared as above for **1**, using **L** (0.518 g, 1.99 mmol) and $AgBF_4$ (0.195 g, 1.0 mmol) to yield a white solid (0.591 g, 82.8%) identified as L_2AgBF_4 (**2**); ^{1}H-NMR (400 MHz, acetone-d_6): δ: 9.13 (dd, J_1 = 1.68, J_2 = 6.0, 1H, *quinoline*); 8.80 (dd, J_1 = 1.32, J_2 = 7.48, 1H, *quinoline*); 8.75 (d, J = 2.84, 1H, 5-*pz*); 8.64 (dd, J_1 = 1.68, J_2 = 8.36, 1H, *quinoline*); 8.51 (dd, J_1 = 1.24, J_2 = 8.24, 1H, *quinoline*); 7.92 (m, 2H, *quinoline* + 3-*pz*); 7.76 (m, 1H, *quinoline*); 6.67 (dd, J_1 = 1.68, J_2 = 2.72, 1H, 4-*pz*); Anal. Calcd. for $C_{24}H_{18}AgBF_4N_6O_4S_2$: C, 40.42; H, 2.54; N, 11.78. Found C, 40.11; H, 2.29; N, 11.52.

Crystal structure determinations

X-ray diffraction intensity data from a colorless bar-shaped crystal of **L**, a colorless needle crystal of **1**, and a colorless chunk of **2** were measured at 150(2) K on a Bruker SMART APEX diffractometer (Mo-Kα radiation, λ = 0.71073 Å).[18] The raw area detector data frames were processed with SAINT+.[18] The reported unit cell parameters were determined by least-squares refinement of 5212, 4595, and 8779 reflections from the data sets of **L**, **1**, and **2**, respectively. Direct methods structure solution, difference Fourier calculations and full-matrix least-squares refinement against F^2 were performed with SHELXTL.[19]

The ligand **L** crystallizes in the triclinic system. The space group $P\bar{1}$ was assumed and confirmed by the successful solution and refinement of the structure. The asymmetric unit consists of one molecule. All non-hydrogen atoms were refined with anisotropic displacement parameters. Hydrogen atoms were placed in geometrically idealized positions and included as riding atoms with refined isotropic displacement parameters.

Compound **1** crystallizes in the space group $P2_1/n$ as determined uniquely by the pattern of systematic absences in the intensity data. The asymmetric unit consists of one $Ag(C_{12}H_9N_3O_2S)_2^+$ cation and one $CF_3SO_3^-$ anion. All non-hydrogen atoms were refined with anisotropic displacement parameters. All hydrogen atoms were located in difference maps before being placed in geometrically idealized positions and included as riding atoms.

Compound **2** crystallizes in the space group $C2/c$ as determined by the pattern of systematic absences in the intensity data and by the successful solution and refinement of the structure. The asymmetric unit consists of one $Ag(C_{12}H_9N_3O_2S)_2^+$ cation, one BF_4^- anion and half of one acetone molecule which is disordered about a two-fold axis of rotation. The disordered acetone was refined isotropically with the aid of C–C and C–O distance restraints. All other non-hydrogen atoms were refined with anisotropic displacement parameters. Non-disordered hydrogen atoms were located in difference maps before being placed in geometrically idealized positions and included as riding atoms. Further details about crystal data collection, and refinement parameters for **L**, **1**, and **2** are collected in Table 1.

Results and discussion

Syntheses and characterization

The pyrazolyl functionalized 8-sulfonyl-quinoline ligand (**C_9H_6N-SO_2-pz**, **L**) was easily prepared (Scheme 1) in one step from 8-quinoline-sulfonyl chloride and pyrazole, under basic conditions (NaH) in dry THF. Removal of NaCl and volatiles produced **L** in 94% yield, as an air and moisture stable white powder, soluble in common organic solvents but insoluble in water and alcohols. Its silver(I) complexes were synthesized in good yield from the reaction between **L** and the corresponding silver salts in THF, Scheme 1, generating compounds with a **L**:Ag ratio of 2:1, as demonstrated by elemental analyses. They are stable white powders, showing decomposition only after several months under daylight, and are soluble in acetone and acetonitrile, but insoluble in chlorinated solvents, diethyl ether, alcohols or water.

The NMR spectrum of the ligand shows the expected set of resonances for the quinoline and pyrazolyl rings. For compounds **1** and **2**, the peaks of the pyrazolyl ring and some of the quinoline moiety are significantly shifted downfield, indicating the coordination of the ligand to the metallic center in solution. Although the X-ray analysis of the crystalline forms of **1** and **2** shows that in the solid state the quinoline and pyrazolyl rings are non-equivalent (*vide infra*), their NMR spectra show equivalent protons, presumably because of fast exchange of the ligands and metals on the NMR time scale. Further, the ^{1}H-NMR spectra of **1** and **2** are indistinguishable, showing that their solution structure is not anion dependent, and suggesting that in solution the structure of the cationic building blocks are identical. This leads to the conclusion that the differences in their solid-state structures appear in the process of crystallization.

Solid-state structures

Single crystals for X-ray crystal structure determination were grown under identical conditions: vapor diffusion of diethyl ether into an acetone solution of the respective compound (**L**, **1** or **2**) at 25 °C. For details about crystal data collection, and refinement parameters see Table 1. Selected bond distances and angles for **L**, **1**, and **2** are given in Table 2.

Crystal structure of L. The asymmetric unit of **L** consists of one molecule; an ORTEP representation of **L**, together with the numbering scheme is shown in Fig. 1. All bond lengths and angles (see Table 2) fall within the normal range found for this type of compound.

The ligand has the N1 pyrazolyl nitrogen atom oriented away from the quinoline nitrogen atom; this configuration is influenced by a concerted set of π–π stacking and C–H···π interactions involving the aromatic moieties, Fig. 2. Two quinoline rings are involved in a π–π stacking interaction (blue line in Fig. 2), with one pyridine ring from one ligand on top of the phenyl ring from a second ligand. The perpendicular distance between the rings is 3.46 Å, with several C–C distances around 3.6 Å. The rings are parallel (dihedral angle between the planes α = 0.0°) and in an offset arrangement, with a slip angle β (formed by the centroid–centroid vector and the ring normal) of 23°. In addition to this interaction, the hydrogen atoms situated at the *para*-position with respect to the quinoline nitrogen atoms are pointed towards two pyrazolyl rings, generating a C–H···π interaction (red line in Fig. 2) with the following geometrical details: H-centroid

Table 1 Crystal data and structure refinement for C_9H_6N-SO_2-pz (**L**), $[(C_9H_6N\text{-}SO_2\text{-}pz)_2]AgOTf$ (**1**), and $[(C_9H_6N\text{-}SO_2\text{-}pz)_2]AgBF_4$ (**2**)

Compound	**L**	**1**	**2**·$\frac{1}{2}(CH_3)_2CO$
Empirical Formula	$C_{12}H_9N_3O_2S$	$C_{25}H_{18}AgF_3N_6O_7S_3$	$C_{25.50}H_{21}AgBF_4N_6O_{4.50}S_2$
FW, g mol^{-1}	259.28	775.50	742.28
Crystal System	Triclinic	Monoclinic	Monoclinic
Space Group	$P\bar{1}$	$P2_1/n$	$C2/c$
T/K	150(2)	150(2)	150(2)
a, (Å)	7.2730(4)	12.7305(6)	25.4562(8)
b, (Å)	8.8712(5)	13.6623(7)	8.5807(3)
c, (Å)	9.7087(5)	16.9108(8)	26.1156(9)
α, (°)	81.238(1)	90	90
β, (°)	70.799(1)	107.898(1)	93.666(1)
γ, (°)	67.737(1)	90	90
V, (Å^3)	547.19(5)	2798.9(2)	5692.8(3)
Z	2	4	8
R_1; $I > 2\sigma(I)$	0.0334	0.0364	0.0352
wR_2; $I > 2\sigma(I)$	0.0852	0.0665	0.0927

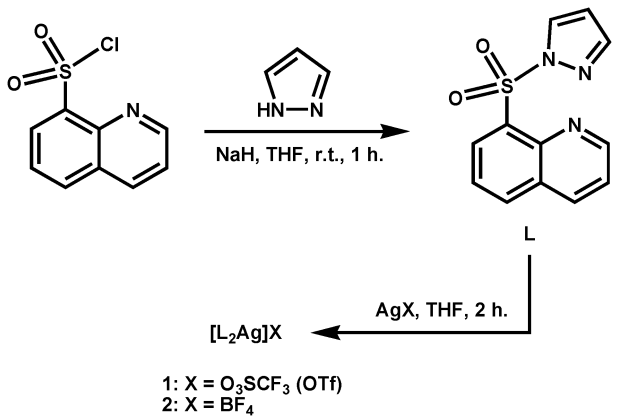

Scheme 1 Synthetic pathway toward the pyrazolyl functionalized 8-sulfonyl-quinoline ligand (**L**) and its silver(I) complexes.

Table 2 Selected bond lengths (Å) and angles (°) for **L**, **1**, and **2**

	L	**1**	**2**·$\frac{1}{2}(CH_3)_2CO$
S(1)–O(2)	1.4278(10)	1.416(2)	1.4251(19)
S(1)–O(1)	1.4275(10)	1.428(2)	1.4234(17)
S(1)–N(2)	1.6758(12)	1.682(3)	1.694(2)
S(1)–C(11)	1.7620(13)	1.764(4)	1.771(2)
Ag(1)–N(1)	—	2.296(3)	2.278(2)
Ag(1)–N(3)	—	2.482(3)	2.4491(19)
Ag(1)–N(4)	—	2.292(3)	2.1966(19)
Ag(1)–N(6)	—	2.501(3)	—
O(2)–S(1)–O(1)	119.85(6)	120.91(16)	122.00(11)
N(1)–Ag(1)–N(4)	—	121.48(11)	135.98(7)
N(3)–Ag(1)–N(4)	—	110.46(10)	132.48(7)
N(1)–Ag(1)–N(3)	—	90.07(10)	87.92(7)
N(4)–Ag(1)–N(6)	—	90.63(10)	—
N(1)–Ag(1)–N(6)	—	112.91(10)	—
N(3)–Ag(1)–N(6)	—	134.77(9)	—

distance = 2.95 Å, C-centroid distance = 3.58 Å and the C–H-centroid angle = 126°.

This interaction forms dimers, that are further associated into chains, through another set of π–π stacking interaction between dimers, with similar characteristics as described above. However, the perpendicular distance between the rings is slightly shorter, at 3.37 Å, compared with the above 3.46 Å. Although not extremely significant (only *ca.* 0.1 Å), this

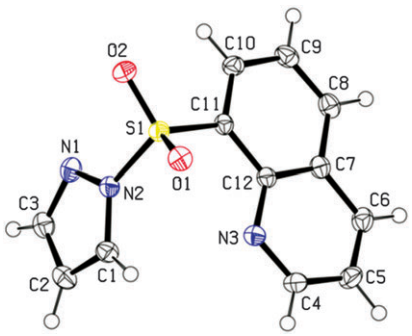

Fig. 1 ORTEP representation of C_9H_6N-SO_2-pz (**L**), with the displacement ellipsoids drawn at the 50% probability level.

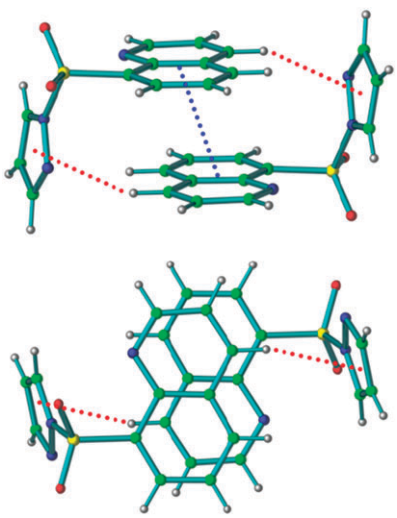

Fig. 2 Dimer formation in the crystal packing of **L**, through a concerted set of π–π stacking (blue line) and C–H···π interactions (red lines).

difference may be influenced by the fact that in the dimer formation there is also a C–H···π interaction involved, while the chain association of the dimers is based solely on π–π stacking interactions. These dimers are further associated into sheets by offset face-to-face π–π stacking interactions between the pyrazole rings that serve as hydrogen acceptors in the

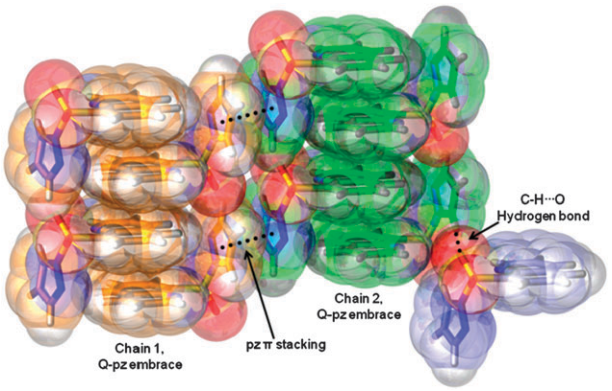

Fig. 3 Space filling representation of the supramolecular association of dimers into a 3D architecture.

embrace synthon. The perpendicular distance between the rings is 3.46 Å, with several C–C and C–N distances around 3.6 Å. The rings are parallel with a dihedral angle between the pyrazolyl planes of 0.0° and a slip angle β of 21°. The sheets are connected in a 3D network by C–H···O weak hydrogen bonds between the acidic 5H atom from a pyrazolyl ring from one sheet and the O atom from a sulfonyl group from an adjacent sheet. This interaction is characterized by a H···O distance of 2.49 Å, a C···O distance of 3.36 Å, and a C–H–O angle of 154°. Fig. 3 shows a space filling representation of the crystal packing of **L**. It should be emphasized that the dimer/chain/sheet/3D association is just a "stepwise" description of the crystal packing of **L**, since these interactions most likely occur simultaneously in the crystallization process.

Crystal structure of $(L_2Ag)O_3SCF_3$ (1). The asymmetric unit of **1** consists of one $(L_2Ag)^+$ cation and one $CF_3SO_3^-$ anion. An ORTEP representation of the cationic unit of **1** and the numbering scheme is shown on the top part of Fig. 4. Significant bond lengths and angles are listed in Table 2. The geometry about the silver is distorted tetrahedral with the large distortions arising from the restricted "bite" angle of the ligand, the $N_{pyrazolyl}$–Ag–$N_{quinoline}$ angles being 90.07° and 90.63°, respectively. A close examination of the structure reveals that the Ag(I) atom is out of both quinoline planes, as can be seen on the bottom part of Fig. 4.

For maximum overlap with the lone pair on the nitrogen donor atom, the metal would lie in the plane of the quinoline ring. Any deviation where the metal lies out of this plane can be measured by the Ag–N–C–C torsion angle. An ideal structural arrangement generated by the "normal" coordination of the nitrogen atom would generate torsion angles that would have a value of 180°. In the case of **1** the torsion angles are as follows: Ag(1)–N(3)–C(12)–C(7) = 158.45° and Ag(1)–N(6)–C(24)–C(19) = 167.84°. This deviation also explains the fact that Ag–$N_{pyrazolyl}$ bond lengths (Ag(1)–N(1) = 2.296(3) Å and Ag(1)–N(4) = 2.292(3) Å) are about 0.2 Å shorter than Ag–$N_{quinoline}$ bond lengths (Ag(1)–N(3) = 2.482(3) Å and Ag(1)–N(6) = 2.501(3) Å, see also Table 2), and might be caused by the limited flexibility of the sulfonyl bridge. The same limited flexibility could be also responsible for the occurrence of two O···Ag contacts shorter than the sum

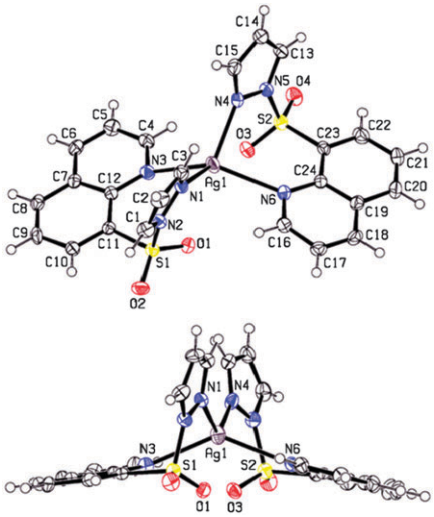

Fig. 4 Top: ORTEP representation of $(L_2Ag)O_3SCF_3$ (**1**), with the displacement ellipsoids drawn at the 50% probability level; bottom: side view of **1** showing the position of the silver(I) atom out of the quinoline plane.

of their van der Waals radii, O(1)–Ag(1) = 2.79 Å and O(3)–Ag(1) = 2.84 Å, but these interactions do not influence the overall structural features of **1**.

As observed with **L**, compound **1** undergoes similar concerted π–π stacking and C–H···π interactions. Two cationic $(L_2Ag)^+$ units are stacked with one pyridine ring from one unit on top of the phenyl ring from a second unit, as pictured by the blue line in Fig. 5. The perpendicular distance between the rings is 3.44 Å, with the quinolines in an almost perfect parallel arrangement; in this case the dihedral angle α (calculated based on a py–ph interaction) is 2.8°, probably because of the torsion imposed by the ligand coordination to the metal center, as described above.

The rings are in an offset orientation, with a slip angle β of 21.6°. A C–H···π interaction (red line in Fig. 5) supports the association of the cationic units of **1**: the hydrogen atoms situated at the *para*-position with respect to the quinoline nitrogen atoms interact with two pyrazolyl rings, generating a pair of C–H···π interactions with the following geometrical details: H-centroid distance = 2.80 Å, C-centroid distance = 3.67 Å and the C–H-centroid angle = 154° and H-centroid distance = 2.95 Å, C-centroid distance = 3.79 Å and the C–H-centroid angle = 148°, respectively. These interactions connect other symmetry related units, thus generating chains running in the *ac* plane of the unit cell. A space filling representation of the extended π–π stacking interactions in **1**, generating infinite chains is pictured in Fig. 6.

The chains are further connected into sheets, *via* hydrogen bonding involving the counter-ions. As shown in Fig. 7 as black dotted lines, each $F_3CSO_3^-$ makes two C–H···O weak hydrogen bonds. The C–H···O interactions, made between adjacent chains, are 2.38 Å and 2.32 Å, respectively, with the corresponding angles of 169 and 176°. While not short contacts (the sum of van der Waals radii of oxygen and hydrogen atoms is 2.68 Å),[20] the bonds are close to linear. As stated for other similar types of such weak interactions, hydrogen bonds that are close to linear indicate a substantial interaction

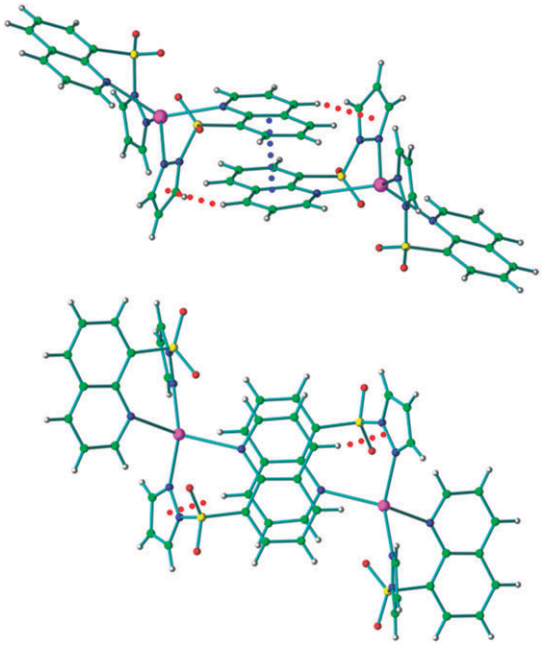

Fig. 5 Self-assembly of two $(L_2Ag)O_3SCF_3$ cationic units through concerted π–π stacking (blue line) and C–H···π interactions (red lines).

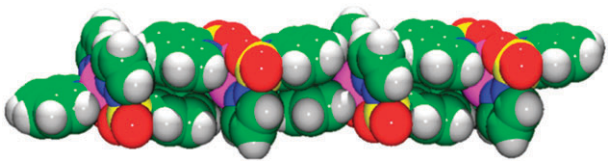

Fig. 6 Space filling representation of a chain in the supramolecular structure of **1**.

between the O and H atoms, even in cases where the distances are close to the sum of the van der Waals radii.[21]

Crystal structure of $(L_2Ag)BF_4$ (2). The asymmetric unit of **2** consists of one $(L_2Ag)^+$ cation, one BF_4 anion and half of one acetone molecule which is disordered about a two-fold axis of rotation. An ORTEP representation of the cationic unit of **2**, and the numbering scheme is shown in Fig. 8, while the most important bond lengths and angles are listed in Table 2. In contrast to **1**, in this compound the silver center is tri-coordinated, with one ligand chelating the metal and with the second acting as a monodentate ligand through its pyrazolyl ring, and having the quinoline moiety oriented away from silver. Hence, the environment about the silver(I) atom is a flattened trigonal pyramid (sum of the N(1)–Ag(1)–N(3), N(3)–Ag(1)–N(4) and N(1)–Ag(1)–N(4) bond angles = 356.38°, see also Table 2), with a significant distortion caused by the restricted angle (87.92°) of the chelating ligand. The BF_4^- counterion is positioned close to the Ag(I) center, with a F(4)–Ag(1) distance of 2.84 Å, too long for the F atom to be coordinated to silver, but suggestive of a non-covalent interaction of the species (the sum of the F and Ag van der Waals radii being 3.29 Å). The limited flexibility of the SO_2 bridge leads to two close contacts between the oxygen and silver(I) atoms (O(1)–Ag(1) = 2.69 Å and O(3)–Ag(1) = 2.94 Å).

As with **L** and **1**, the cationic units in **2** are associated into dimers by similar π–π stacking/C–H···π interactions, see Fig. 9, blue and red lines, respectively. In this case, the difference is that the π–π stacking occurs mainly between the phenyl rings of the quinoline, (see the bottom part of Fig. 9). The quinoline rings are in a parallel arrangement, with the dihedral angle $\alpha = 0.0°$ and a perpendicular distance between the rings of 3.49 Å. The phenyl rings are also parallel displaced, with a slip angle β of 25.7°. Another difference between **2** and the above **L** and **1** is that the C–H···π interaction that accompanies the π–π stacking interaction involves hydrogen atoms situated on the *para*-position with respect to the sulfonyl group of the quinoline moiety. The metrical parameters for this interaction are as follows: H-centroid distance = 3.09 Å, C-centroid distance = 3.98 Å and the C–H–centroid angle = 156°.

This combined set of interactions generates dimers, pictured in the top of Fig. 10 as a space filling representation. Another significant difference found in the crystal packing of **2** is that the dimers are not further self-assembled in chains, as observed with **1**, through additional π–π stacking/C–H···π interactions. As pictured in the bottom part of Fig. 10, an acetone molecule is sandwiched between two uncoordinated quinoline rings, therefore hampering the π–π stacking/C–H···π interactions of these two moieties.

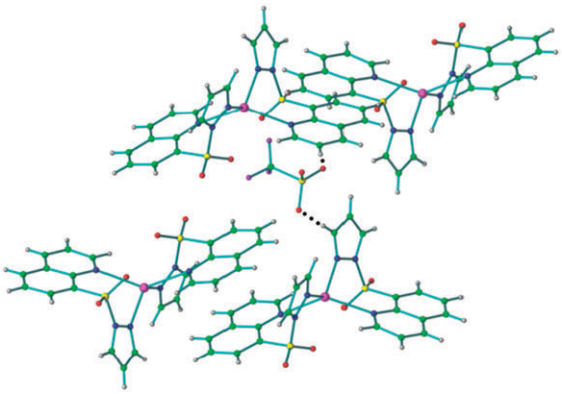

Fig. 7 Hydrogen bonding (black dotted lines) between two dimers in the crystal packing of **1**.

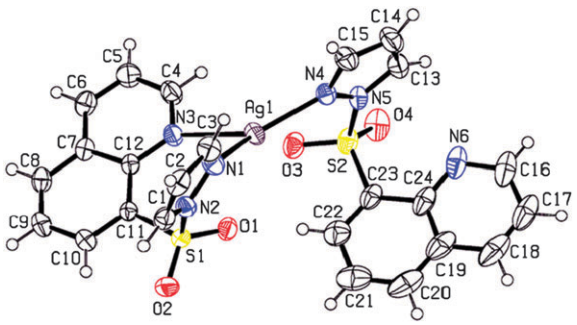

Fig. 8 ORTEP representation of $(L_2Ag)BF_4$ (**2**), with the displacement ellipsoids drawn at the 50% probability level.

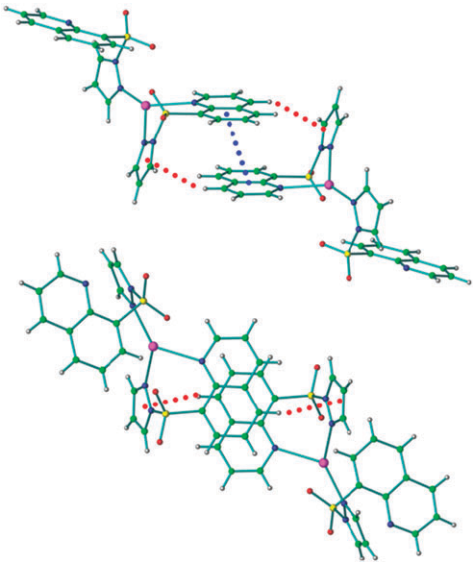

Fig. 9 Self-assembly of two $(L_2Ag)BF_4$ cationic units through concerted π–π stacking (blue line) and C–H···π interactions (red lines).

Statistical investigation of the 8-substituted quinoline π–π stacking synthon

The common denominator of all these structures is the association of the ligand and its silver(I) complexes through π–π stacking interactions of the quinoline rings. The presence of the pyrazolyl rings in an appropriate position with respect to the quinoline rings makes possible the presence of additional C–H···π interactions between the already stacked moieties. These interactions generate dimers in all cases, and in two cases (**L** and compound **1**) the dimers undergo further self-assembly into chains, again based on π–π stacking interactions. When a suitable counter-ion is present, its involvement in the crystal packing was also observed.

One major difference between the stacked structures of **L** and **1** on one hand and **2** on the other is the overlap of the quinoline rings. In the case of **L** and **1** the major overlap occurs between the pyridine and phenyl rings, while in the case of **2** the overlap involves mainly the phenyl groups of the quinoline moiety, with the pyridine rings being oriented away from one another (compare Fig. 2 and 5 with Fig. 9). In order to determine whether such an interaction (the π–π stacking of two quinoline rings) was either found only in isolated examples or was representative of a common framework, to point out some particulars (*i.e.* what rings undergo the major overlap) associated with this interaction and also to determine the influence of additional non-covalent forces over the "main" π–π stacking interaction of the quinoline rings, a Cambridge Structural Database (CSD)[22] search has been performed using the 5.30 version of the CSD (November 2008, plus two updates), *via* the ConQuest 3D routine.[23] The results were analyzed using the CSD VISTA program.[24] Although other statistical analyses of π–π stacking interactions based on pyridine and similar ligands are present in the literature,[10b] we were specifically interested in analyzing only structures containing the quinoline ring functionalized at its 8-position with other possible donor groups. Therefore, in the first step of our investigation we identified all compounds containing a quinoline ring having any non-metal substituent (NM) at the 8th position, which in turn has a second non-metal atom bonded to it. Further, the nitrogen atom of the quinoline ring was allowed to be coordinated to any metal (4M). As such, we excluded the well known class of metal complexes of 8-HO-quinoline and 8-HS-quinoline and also compounds where quinoline acts only as an additional ligand in the preparation of adducts with nitrogen containing ligands. This search yielded a subset of 492 crystal structures with an *R* factor <0.1, which was used in the next step of our analysis.

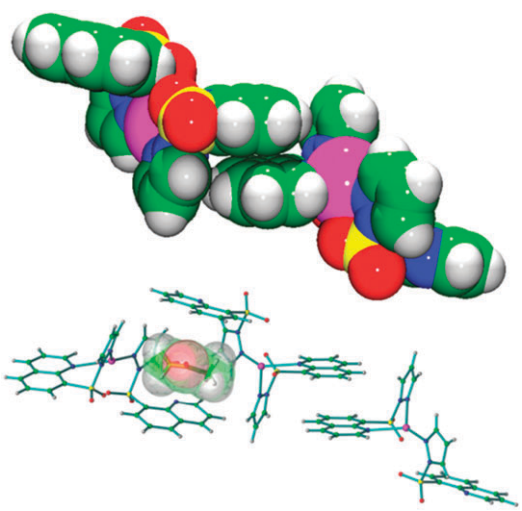

Fig. 10 Top: space filling representation of a dimer of **2**; bottom: an acetone molecule (in space filling representation) sandwiched between two uncoordinated quinoline moieties.

Further restrictions on the database search then followed from the geometric parameters given in Scheme 2 and from accepted values for π–π interactions. Considering an extreme case of a small overlap between two rings of the quinoline system, with the other two rings oriented away one from another, as depicted in Scheme 2a, a maximum centroid–centroid distance of 7.3 Å was considered,[25] to encompass either intra- or intermolecular π–π stacking interactions involving the quinoline groups. As shown further in Scheme 2b, to gather meaningful results for a π–π stacking interaction, the dihedral plane α between the stacked rings was restricted to values between 0° and 5°. The parallel displacement of the rings was measured by the angle β formed between the centroid–centroid vector and the ring normal to the corresponding aromatic plane, and was allowed to have values from 0° to 90°.

From these combined restraints, 314 crystal structures from the previously obtained subset of 492 (or 69%) were found to contain a quinoline π–π stacking interaction. Since some of the entries contained more than one example of such an interaction, these 314 entries generated 592 examples of the motif.

The discussion of the geometric parameters associated with this interaction utilizes all these 592 examples. The results of the search show that the vast majority of quinoline–quinoline plane contacts are parallel or close to parallel to each other, *i.e.* the dihedral angle α is zero or near zero. In fact, 434 hits out of 592 (73%) have values for α between 0.0° and 0.04° (see Fig. 11), with the rest equally spread up to 5°.

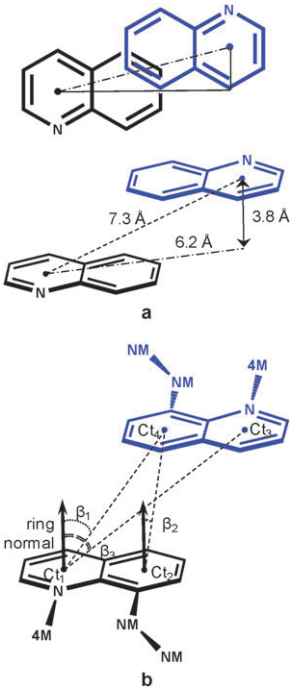

Scheme 2 Geometric parameters associated with the CSD search: NM = non-metal, 4M = any metal, Ct_i = ring centroid, β = angle between the ring normal and centroid–centroid vector; the Ct–Ct distances were constrained to an intra- or intermolecular contact between 3.0 and 7.3 Å; the dihedral angle between the stacked quinoline rings (α, not pictured) was allowed to range from 0.0 up to 5.0°; the displacement of the quinoline rings was measured by β, allowed to vary between 0° and 90°.

Regardless of the nature of the overlapping rings (pyridine over pyridine, phenyl over phenyl or pyridine over phenyl), the centroid–centroid contacts between two aromatic fragments start around 3.2–3.4 Å and have a maximum in the number of occurrences slightly below 3.8 Å, as pictured in Fig. 12. However, the histograms show that all three contacts could be found, with a higher preference for pyridine–phenyl interactions, followed by phenyl–phenyl contacts and ending with pyridine–pyridine interactions.

For phenyl–pyridine interactions, after reaching a maximum around 3.8 Å, the number of occurrences decreases as the centroid–centroid distance increases, while both phenyl–phenyl and pyridine–pyridine contacts show a spike in the number of occurrences around 5.2 and 6.8 Å. This difference is explained by the fact that a close pyridine–phenyl contact (a small Ct1–Ct4 distance) would also impose short Ct2–Ct4 and Ct1–Ct3 distances, while a short Ct2–Ct4 or Ct1–Ct3 distance (with the pyridine or phenyl rings oriented away one from another), would entail a long Ct1–Ct3 or Ct2–Ct4 distance, respectively (see Scheme 2b).

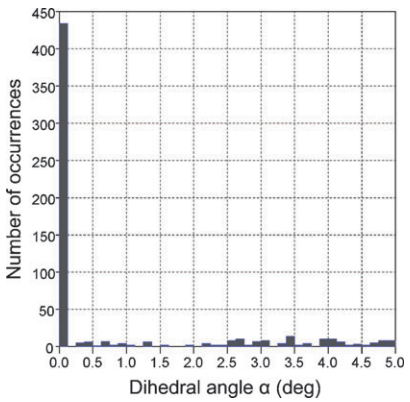

Fig. 11 Distribution in dihedral angle α (°) between mean planes of quinoline rings involved in the π–π interaction.

Also, regardless of the nature of the aromatic rings, they are parallel displaced with respect to each other. Fig. 13 shows the histogram of the displacement angles $\beta1$, $\beta2$, and $\beta3$, as they were defined in Scheme 2b, and Fig. 14 shows scattergrams for the correlation between the displacement angles and the corresponding centroid–centroid distances. The average values for slip angles are 32° for $\beta1$ and 44° for $\beta2$ and $\beta3$, and they all reveal a common trend toward smaller displacement angles (smaller β values) as the centroid–centroid distance decreases. In all cases, for centroid–centroid distances up to 3.8 Å the displacement angle lies around 25°.

Selected examples from the literature

The results of this search show that 69% of the 8-functionalized quinoline based ligands undergo π–π stacking interactions. A manual inspection of the hits showed that the π–π stacking interactions are often accompanied by additional interactions, encompassing C–H···π interactions like with **L** and compounds **1** and **2**, or weak hydrogen bonds of the type C–H···A (where the hydrogen acceptor could be part of the stacked supramolecular assembly or a counterion). Examples where the π–π stacking interaction of the quinoline moieties was unsupported by additional interactions were also found.

In the following, we present several descriptive structures (figures of the compounds presented as ESI†) of the main motifs that we identified, systematized as follows: first, we considered the case of those stacking interactions where the main overlap of the quinoline rings occurred between phenyl and pyridine rings. Within this general case, we treated first some of the examples where the stacking interactions were supported by concerted C–H···π interactions (Scheme 3 and Fig. S1†), as in our compounds described above, followed by additional C–H···A hydrogen bonds or unsupported π–π stacking interactions between the quinoline rings (Scheme 4 and Fig. S2†). Examples of π–π stacking interactions where the overlap occurs mainly between two pyridine (Scheme 5 and Fig. S3†) and phenyl rings (Scheme 6 and Fig. S4†) of the quinoline system are described next, followed by some examples of unconventional stacking of the quinoline rings (Scheme 7 and Fig. S5†), and ending with examples of compounds where the stacking interactions do not occur (Scheme 8 and Fig. S6†), showing some of the reasons why this quinoline synthon is precluded. The captions of each Scheme contain important geometric parameters associated with the interactions that were identified. For π–π stacking interactions the following are given: centroid–centroid distance (Ct–Ct), the perpendicular distance between the rings (⊥) and the slip angle β. Additional C–H···π interactions and weak C–H···Acceptor hydrogen bonds are characterized by

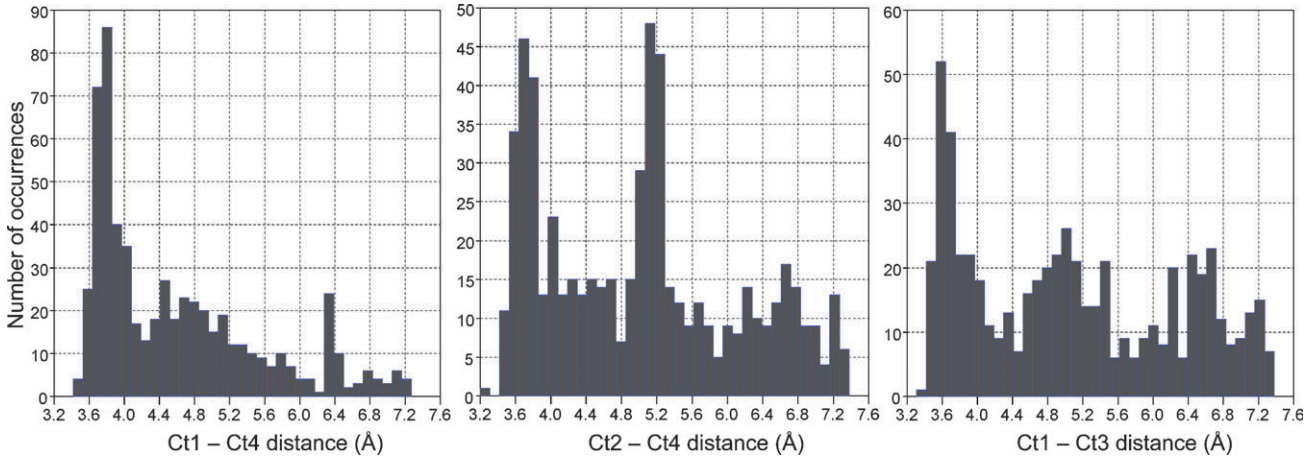

Fig. 12 Histogram for the centroid–centroid distances (Å) between two quinoline rings as outlined in Scheme 2.

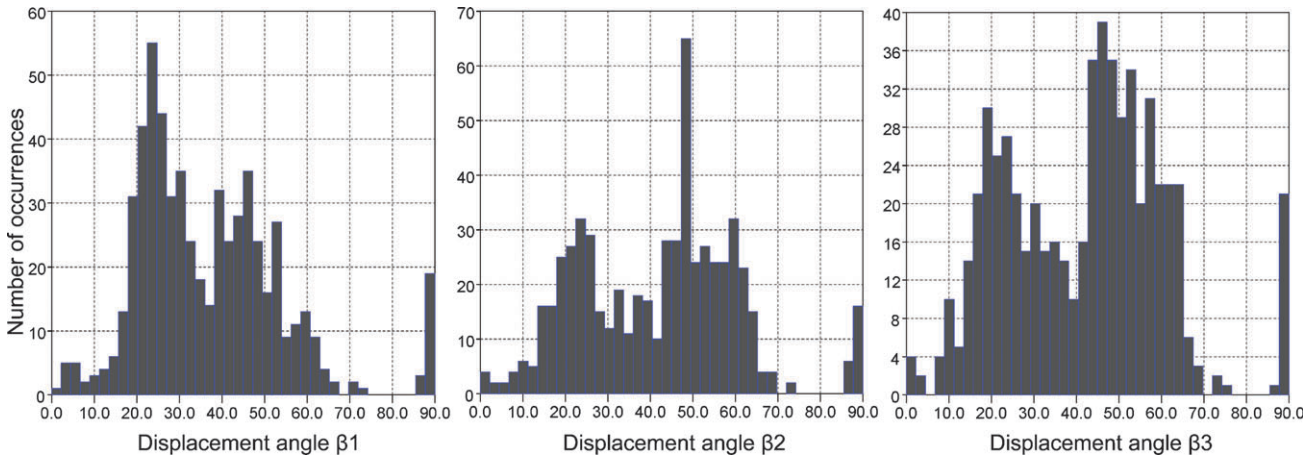

Fig. 13 Histogram of displacement angles β (°) between quinoline planes in the π–π interaction.

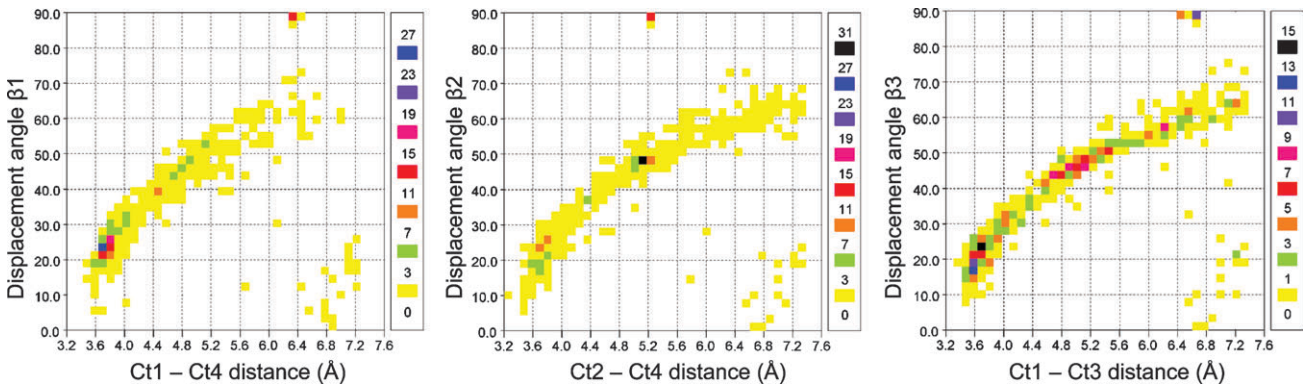

Fig. 14 Scattergram for a correlation between the displacement angle (β) and the centroid–centroid distance (Ct–Ct) as outlined in Scheme 2.

H-centroid (H–Ct) distance and C–H-centroid (C–H–Ct) angle, and H···Acceptor (H–A) and C–H–Acceptor (C–H–A) angles, respectively. These data were calculated using the .cif files downloaded from the CSD database and the program PLATON.[26] While the examples presented here do not offer an exhaustive coverage of all quinoline based compounds that undergo π–π stacking interactions, they should offer enough information for the reader to evaluate the important cases of quinoline π–π stacking accompanied (or not) by other interactions, and, therefore, the usefulness of the quinoline synthon in supramolecular chemistry and crystal engineering.

The π–π stacking in bis(4-fluoro-*N*-(quinolin-8-yl)benzenesulfonamidato-*N*,*N*′)-zinc(II) (ADEHOH),[27] is supported by additional C–H···π interactions involving the hydrogen atom situated in the *para* position (4-position) with respect to the nitrogen atom of the quinoline ring. In addition, another

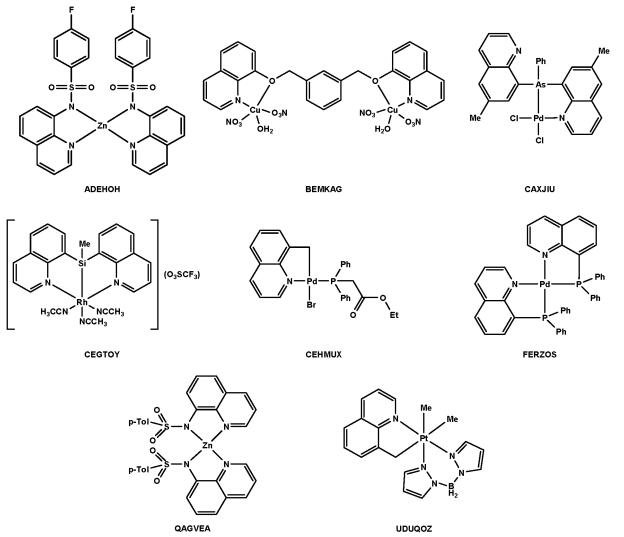

Scheme 3 Refcodes and descriptive structures of quinoline based compounds that undergo a phenyl–pyridine π–π stacking supported by additional C–H···π interactions: ADEHOH: Ct–Ct = 3.6 Å, ⊥ = 3.5 Å, β = 18°, H–Ct = 2.74 Å, C–H–Ct = 153°, H–O = 2.71 Å, C–H–O = 162°; BEMKAG: Ct–Ct = 3.9 Å, ⊥ = 3.5 Å, β = 6°, H–Ct = 2.72 Å, C–H–Ct = 156°; CAXJIU: Ct–Ct = 3.7 Å, ⊥ = 3.7 Å, β = 6°, H–Ct = 2.76 Å, C–H–Ct = 145°; CEGTOY: Ct–Ct = 3.7 Å, ⊥ = 3.6 Å, β = 20.8°, H–Ct = 2.93 Å, C–H–Ct = 165°, H–Ct = 2.55 Å, C–H–Ct = 169°; CEHMUX: Ct–Ct = 3.7 Å, ⊥ = 3.6 Å, β = 21.1°, H–Ct = 2.88 Å, C–H–Ct = 166°; FERZOS: Ct–Ct = 3.7 Å, ⊥ = 3.5 Å, β = 19.0°, H–Ct = 2.69 Å, C–H–Ct = 164°; QAGVEA: Ct–Ct = 3.56 Å, ⊥ = 3.4 Å, β = 18.5°, H–Ct = 2.75 Å, C–H–Ct = 141°; UDUQOZ: Ct–Ct = 3.7 Å, ⊥ = 3.5 Å, β = 22.6°, H–Ct = 2.66 Å, C–H–Ct = 175°; see Fig. S1† for pictorial representations of the interactions.

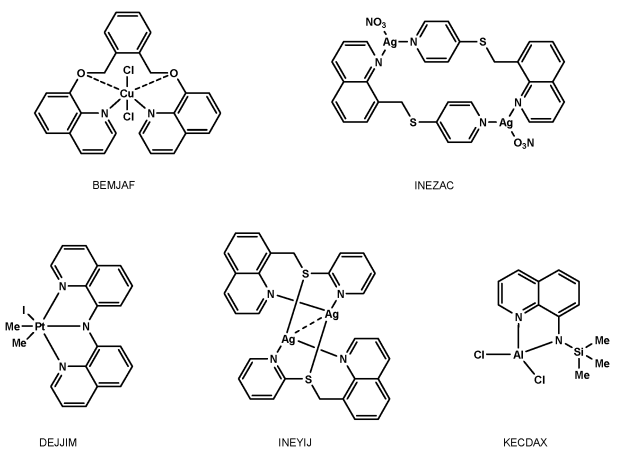

Scheme 4 Refcodes and descriptive structures of quinoline based compounds that undergo a phenyl–pyridine π–π stacking in combination with C–H···A hydrogen bonds (top) and unsupported phenyl–pyridine π–π stacking (bottom); BEMJAF; Ct–Ct = 3.7 Å, ⊥ = 3.4 Å, β = 28.8°, H–Cl = 2.91 Å, C–H–Cl = 144°, H–Cl = 2.73 Å, C–H–Cl = 150°; INEZAC; Ct–Ct = 3.7 Å, ⊥ = 3.6 Å, β = 19.6°, H–O = 2.6 Å, C–H–O = 140°, H–O = 2.7 Å, C–H–O = 146°; DEJJIM; Ct–Ct = 3.7 Å, ⊥ = 3.4 Å, β = 23.9°; INEYIJ; Ct–Ct = 3.8 Å, ⊥ = 3.5 Å, β = 24.5°; KECDAX; Ct–Ct = 3.4 Å, ⊥ = 3.3 Å, β = 15.3°; see Fig. S2† for pictorial representations of the interactions.

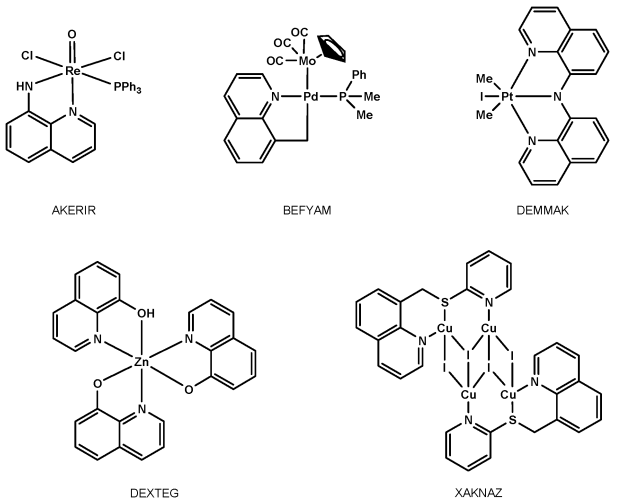

Scheme 5 Refcodes and descriptive structures of quinoline based compounds that undergo a pyridine–pyridine π–π stacking; AKERIR; Ct–Ct = 3.6 Å, ⊥ = 3.5 Å, β = 20.1°, H–Cl = 3.1 Å, C–H–Cl = 139°, H–Cl = 2.9 Å, C–H–Cl = 144°; BEFYAM; Ct–Ct = 3.6 Å, ⊥ = 3.4 Å, β = 21.4°, H–O = 2.6 Å, C–H–O = 143.8°; DEMMAK; Ct–Ct = 3.4 Å, ⊥ = 3.4 Å, β = 16°, H–Ct = 2.7 Å, C–H–Ct = 171°; DEXTEG; Ct–Ct = 3.6 Å, ⊥ = 3.4 Å, β = 20.2°, H–Ct = 2.5 Å, C–H–Ct = 165°; XAKNAZ; Ct–Ct = 3.7 Å, ⊥ = 3.4 Å, β = 23.1°; see Fig. S3† for pictorial representations of the interactions.

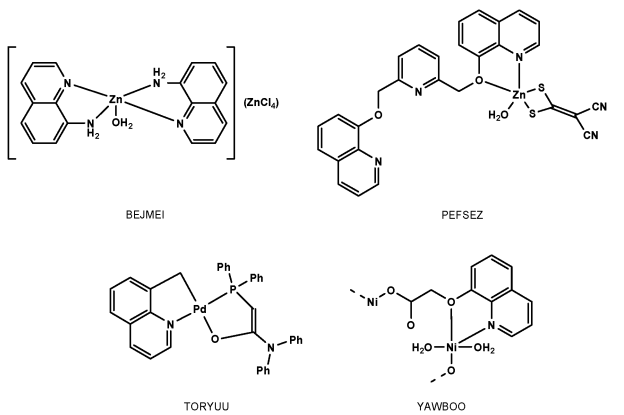

Scheme 6 Refcodes and descriptive structures of quinoline based compounds that undergo a phenyl–phenyl π–π stacking; BEJMEI; Ct–Ct = 3.7 Å, ⊥ = 3.5 Å, β = 21.7°, H–Cl = 2.89 Å, C–H–Cl = 178°; PEFSEZ; Ct–Ct = 3.5 Å, ⊥ = 3.4 Å, β = 15.4°; TORYUU; Ct–Ct = 3.6 Å, ⊥ = 3.5 Å, β = 12.7°; YAWBOO; Ct–Ct = 3.7 Å, ⊥ = 3.5 Å, β = 19.9°; see Fig. S4† for pictorial representations of the interactions.

hydrogen atom from the quinoline ring (5-position) is involved in a C–H···O weak hydrogen bond with the sulfonamide group. (1,3-Bis(8-quinolyloxymethyl)benzene)-diaqua-tetranitrato-di-copper(II) (BEMKAG),[28] has a similar supporting C–H···π interaction, again involving the hydrogen atom situated in the *para* position with respect to the nitrogen atom of the quinoline ring, which is interacting with the aromatic cloud of the central benzene ring. Dichloro-(bis(6-methyl-quinolinyl)-phenylarsine)-palladium(II) (CAXJIU),[29] undergoes a similar additional interaction involving the same hydrogen atom that interacts with phenyl group bonded to the arsenic.

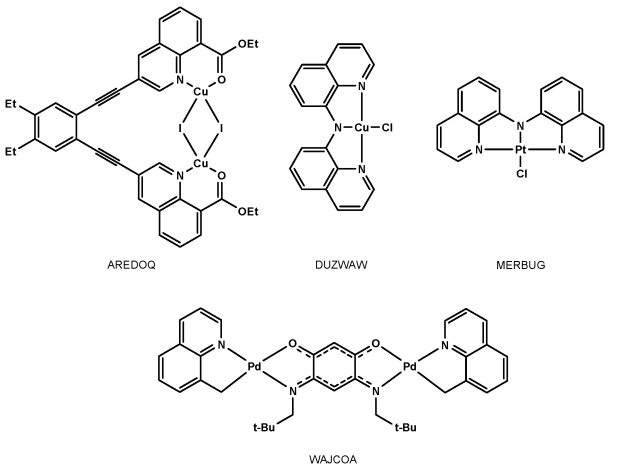

Scheme 7 Refcodes and descriptive structures of quinoline based compounds that undergo an unconventional π–π stacking; AREDOQ; Ct–Ct = 3.6 Å, ⊥ = 3.4 Å, β = 20.2°; DUZWAW; Ct–Ct = 4.5 Å, ⊥ = 3.5 Å, β = 39.5°; MERBUG; Ct–Ct = 3.6 Å, ⊥ = 3.3 Å, β = 22.7°; WAJCOA; no quinoline interaction observed; Ct–Pd = 3.7 Å, ⊥ Pd–Arene distance = 3.5 Å; see Fig. S5† for pictorial representations of the interactions.

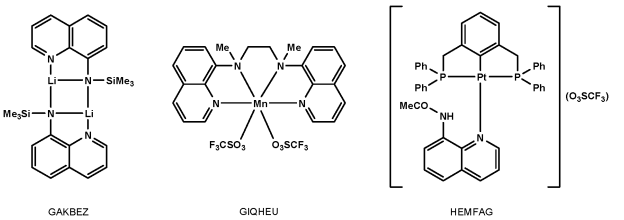

Scheme 8 Refcodes and descriptive structures of quinoline based compounds that do not undergo any π–π stacking; see Fig. S6† for pictorial representations of the interactions.

(Bis-(8-quinolyl)(methyl)silyl)-*tris*-(acetonitrile)-rhodium-bis-(trifluoromethane-sulfonate) (CEGTOY),[30] has two C–H···π interactions, with two of the H atoms (4- and 5-positions) from the stacked quinoline rings oriented toward a non-stacked quinoline ring, generating an interaction similar to other quadruple arene embrace motifs.[4–7] In contrast to ADEHOH, BEMKAG, and CAXJIU, bromo-(ethyl-(diphenylphosphino)-acetate)-(8-quinolinylmethyl)-palladium (CEHMUX),[31] the hydrogen atom involved in the additional C–H···π interaction is situated in the 5-position of the quinoline ring. The next two examples, bis((8-quinolyl)diphenylphosphine-*N*,P)-palladium(II) dichloride dichloromethane solvate monohydrate (FERZOS),[32] and bis((*N*-quinolinyl)toluenesulfonamide)-zinc(II) (QAGVEA),[33] participate in the additional C–H···π interaction again with the hydrogen atom situated in the *para* position with respect to the nitrogen atom of the quinoline ring. In dimethyl-(bis(pyrazolyl)-borate)-(8-quinolinylmethyl-C,N)-platinum(IV) (UDUQOZ),[34] the hydrogen atom in the 5-position interacts with the aromatic cloud of a pyrazolyl ring.

Dichloro-(1,2-bis(8-quinolyloxymethyl)benzene)–copper(II) (BEMJAF),[28] has an additional bifurcated C–H···Cl weak hydrogen bond with one chlorine atom that is coordinated to the copper center, while bis((8-(4-pyridylsulfanylmethyl)-quinoline)-(nitrato–O)-silver(I)) (INEZAC),[35] forms two separate C–H···O weak hydrogen bonds with two different oxygen atoms from the NO_3^- counter-ion. In contrast, the crystal packing of dimethyl-iodo-(bis(8-quinolinyl)amido-*N*,*N*′,*N*′′)-platinum(IV) (DEJJIM),[36] bis(8-(2-pyridylsulfanyl-methyl)quinoline)-di-silver(I) diperchlorate (INEYIJ),[35] and dichloro-(8-(trimethyl-silyl)aminoquinoline-*N*,*N*′)-aluminium (KECDAX),[37] is based solely on π–π stacking interactions: as can be seen in Fig. S2†, there are no additional interactions for these compounds.

When the main overlap of the quinoline rings occur between two pyridine rings, one can also find all three cases described above: π–π stacking with additional C–H···π interactions and C–H···A weak hydrogen bonds and unsupported stacking of the quinoline rings. In the case of dichloro-oxo-triphenyl-phosphine-(2-methylquinolinyl-amido)-rhenium(V) (AKERIR),[38] and (dimethylphenylphosphine)-tricarbonyl-(η^5-cyclopenta-dienyl)-molybdenum-(8-methyl-quinoline-C,N)-palladium(II) (BEFYAM),[39] there are additional C–H···A weak hydrogen bonds: in the former there is a bifurcated hydrogen bond with a Cl atom bonded to a Re center acting as a proton acceptor, with the hydrogen atoms from the 4- and 5-positions of the quinoline ring. The latter example involves the 5-hydrogen atom of the quinoline ring and a carbonyl group on the molybdenum atom. The next two examples, dimethyl-iodo-(bis(8-quinolinyl)amido-*N*,*N*′,*N*′′)-platinum(IV) (DEMMAK),[36] and (8-quinolinol-*N*,*O*)-bis(8-quinolinolato-*N*,*O*)-zinc(II) (DEXTEG),[40] the additional interactions are C–H···π interactions, involving mainly the hydrogen atom situated in the *para* position (4-position) with respect to the nitrogen atom of the quinoline ring. An example of unsupported quinoline π–π stacking is provided by bis((iodo)-(iodo)-(8-(2-pyridylsulfanyl-methyl)-quinoline-*N*,*N*′*S*)-di-copper(I)) (XAKNAZ).[41]

In the case of bis(8-aminoquinoline)-aqua-zinc(II) tetra-chloro-zinc(II) (BEJMEI),[42] there is an additional C–H···Cl hydrogen bond, involving the hydrogen atom situated in the *para* position (4-position) with respect to the nitrogen atom of the quinoline ring and a chlorine atom from the $ZnCl_4^{2-}$ counter-ion. The rest of the examples, aqua-(1,1-dicyano-ethylene-2,2-dithiolato)-(bis(quinolyloxymethyl)-pyridine)-zinc(II) (PEFSEZ),[43] (diphenylphosphino-1-diphenyl-amino-ethenyl-oxy)-(methylquinoline)-palladium (TORYUU),[44] and the coordination polymer [(8-quinolyloxyacetato)-diaqua-nickel(II) chloride (YAWBOO),[45] contain unsupported π–π stacking interactions of the quinoline rings.

The π–π stacking interaction in bis(iodo)-(4,5-diethyl-1,2-bis(3-(ethynyl)-8-ethoxycarbonyl-quinoline)benzene)-di-copper(I) (AREDOQ),[46] involve the overlap of a phenyl group from one quinoline ring over an entire quinoline moiety from another molecule. In a similar interaction, chloro-(bis(8-quinolinyl)-amino-*N*,*N*′,*N*′′)-copper(II) (DUZWAW),[47] has one pyridine ring from one unit overlapping the entire quinoline ring from another, with several C–C distances ranging from 3.5 to 3.6 Å and with a N–Cu distance of 3.1 Å. Another example of such an interaction is chloro-(bis(8-quinolinyl)amido-*N*,*N*′,*N*′′)-platinum (MERBUG),[48] with C–C distances from 3.4 Å to 3.6 Å and a N–Pt distance of 3.7 Å. (2-Neopentylamino-5-hydroxy-*N*-neopentyl-*p*-benzoquinone-monoimine)-bis(8-methyl-quinoline-C,N)-di-palladium(II) (WAJCOA),[49] is better described as a Pd–quinoline (M–π) interaction, rather than a quinoline–quinoline π–π stacking; in fact, the quinoline rings are not

overlapping at all, but since the two building blocks are stacked one on top of another, we preferred to present this example here rather than in the following section, where no stacking is observed. Data retrieved from the PLATON analysis of this compound revealed a ⊥ Pd–Arene distance of 3.5 Å, with two "short" Pd–C distances of 3.6 Å.

From the examples found without any π–π stacking interactions we present here only three significant examples: bis((8-trimethylsilylaminoquinoline)-lithium) (GAKBEZ),[50] (*N*,*N*′-dimethyl-*N*,*N*′-bis(8-quinolyl)ethane-1,2-diamine)-bis-(trifluoromethanesulfonato)-manganese(II) (GIQHEU),[51] and (8-acetamidoquinolinato-*N*)-(2,6-bis(diphenylphosphino-methyl)-phenyl-C,P,P′)-platinum triflate (HEMFAG).[52] In all cases, bulky groups (either organic moieties grafted onto the ligand or voluminous counter-ions coordinated to the metallic center) hamper the appearance of the quinoline π–π stacking motif.

The data above show that the π–π stacking of the quinoline groups influence the metrics of the additional interactions. Focusing on the cases where the π–π stacking of the quinoline rings is supported by additional C–H···π interactions, one can identify several subclasses of this motif, based on the type of the H-acceptor aromatic ring (another quinoline moiety, a phenyl ring or other aromatic groups) and the position of that particular ring within the molecule (attached either to the first or to the second NM atom), Scheme 9. By imposing further restraints defining a C–H···π interaction[53] onto the 314 structures found earlier, 22 examples for the first case and 15 examples of the latter were identified.

Data analysis of the geometry of these associated C–H···π interactions is in agreement with results obtained for other weak hydrogen bonding interactions [*i.e.* C–H···X (X = O, N, F, π cloud)]; that is, as the C–H···X (where X in this case is the centroid of a phenyl ring) length decreases, the associated C–H-centroid angles approaches 180°.[54] The histograms for the C–H–Ct angle and for the H–Ct distances and scattergrams for a correlation between the C–H–Ct angle and H–Ct distance are presented as ESI†, Fig. S7 and S8, showing the influence of the quinoline π–π stacking over the C–H···π interaction. An ideal C–H···π interaction would be such that the donor–hydrogen–acceptor angle would be 180°, but the observed values are less than this ideal value. While Fig. S7 and S8 show that the C–H-centroid angle increases as the H–Ct distance decreases, however this trend is smaller than in other cases[54] because of the presence of the π–π stacking between the quinoline rings.

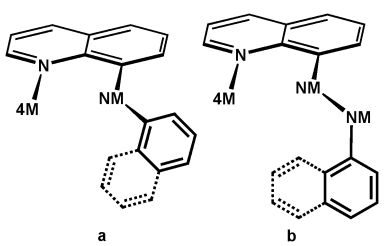

Scheme 9 General structures of substituted quinoline rings that could undergo additional C–H···π interactions: (a) the quinoline_NM_Ph case and (b) the quinoline_NM_NM_Ph case.

Conclusions

In the three new structures presented here, the building blocks were associated by cooperative π–π and C–H–π interactions, involving quinoline and pyrazolyl rings, thus generating dimers and, in two cases, infinite chains. These structures fit into the general description of interactions that we suggest are named heteroaryl embraces, where multiple interactions occur between different aromatic rings. A search of the Cambridge Crystallographic Database showed that this interaction is relatively common for metal complexes of quinoline based ligands. At its simplest level, such an interaction between the building blocks will yield discrete dimeric species. Higher dimensionality networks might be obtained by the extension of the π–π stacking interaction, as in the case of **L** and **1**, or by bringing into play other supramolecular synthons, such as hydrogen bonds.

While the data contained within this paper serves to demonstrate the viability of the "basic" quinoline π–π stacking as a synthon for the construction of supramolecular edifices, certainly the examples presented here serve as a useful example of the importance to the solid state structures of other non-covalent interactions (C–H···π interactions or weak hydrogen bonds) in the organization of species containing such ligands. It should be emphasized that the existence of quinoline moieties within a chemical species is insufficient to guarantee that a π–π stacking will be observed, as the framework was found in only 69% of the structurally characterized cases, depending on the absence or the presence of bulky co-ligands or counter-ions, respectively.

The understanding of intra- and intermolecular forces and of the supramolecular self-assembly process is a prerequisite for the progress of crystal engineering. In this respect, the study of systems like the one presented here is not only of academic interest, but may serve as the basis for the rational design of new solid materials with promising useful properties. Ligands based on functionalized quinolines are appealing because they show a great structural diversity that is derived from their ability to exhibit various coordination patterns combined with their potential to participate in a variety of non-covalent interactions.

The aim of this work was to not only ascertain the influence of the π–π stacking on the outcome of supramolecular structures in a given system, but to show that even in a system where a simple quinoline based ligand is involved, other factors such as the presence of other non-covalent interactions can change the resulting molecular and supramolecular structure. Further studies are clearly needed in order to ascertain the influence of *all* factors on the outcome of a supramolecular array if one hopes to fully control the self-assembly process and thus, to create crystals that exhibit useful properties.

Acknowledgements

Acknowledgements are made to the Donors of the American Chemical Society Petroleum Research Fund for partial support of this research. Also, partial financial support from Eastern Illinois University through a CFR seed grant is greatly appreciated.

Notes and references

1 (*a*) D. J. Braga, *J. Chem. Soc., Dalton Trans*., 2000, 3705; (*b*) G. R. Desiraju, *Angew. Chem., Int. Ed*., 2007, **46**, 8342; (*c*) G. R. Desiraju, *Crystal Engineering—The Design of Organic Solids*, Elsevier, Amsterdam, 1989; (*d*) D. Braga, F. Grepioni and G. R. Desiraju, *Chem. Rev*., 1998, **98**, 1375; (*e*) A. J. Blake, N. R. Champness, P. Hubberstey, W. S. Li, M. A. Withersby and M. Schroder, *Coord. Chem. Rev*., 1999, **183**, 117; (*f*) D. Braga, G. R. Desiraju, J. Miller, A. G. Orpen and S. Price, *CrystEngComm*, 2002, **4**, 500; (*g*) M. D. Hollingsworth, *Science*, 2002, **295**, 2410; (*h*) L. Brammer, *Chem. Soc. Rev*., 2004, **33**, 476; (*i*) M. W. Hosseini, *CrystEngComm*, 2004, **6**, 318; (*j*) D. Braga, L. Brammer and N. Champness, *CrystEngComm*, 2005, **7**, 1; (*k*) G. R. Desiraju, *The Crystal as a Supramolecular Entity. Perspectives in Supramolecular Chemistry*, Wiley, Chichester, UK, 1996, vol. 2; (*l*) D. Braga and F. Grepioni, *Acc. Chem. Res*., 2000, **33**, 601; (*m*) D. Braga and F. Grepioni, *Chem. Commun*., 2005, 3635; (*n*) G. R. Desiraju, *Angew. Chem., Int. Ed. Engl*., 1995, **34**, 2311; (*o*) G. R. Desiraju, *Chem. Commun*., 1997, 1475.

2 See for example: (*a*) D. Braga, L. Maini, M. Polito, E. Tagliavini and F. Grepioni, *Coord. Chem. Rev*., 2003, **246**, 53; (*b*) G. R. Desiraju, *Acc. Chem. Res*., 2002, **35**, 565; (*c*) B. Moulton and M. J. Zaworotko, *Chem. Rev*., 2001, **101**, 1629; (*d*) G. R. Desiraju, *J. Chem. Soc., Dalton Trans*., 2000, 3745; (*e*) A. M. Beatty, *Coord. Chem. Rev*., 2003, **246**, 131; (*f*) A. M. Beatty, *CrystEngComm*, 2001, **3**(51), 243; (*g*) L. J. Brammer, *Dalton Trans*., 2003, 3145.

3 F. H. Allen, W. D. S. Motherwell, P. R. Raithby, G. P. Shields and R. Taylor, *New J. Chem*., 1999, **23**, 25.

4 I. G. Dance and M. L. Scudder, *J. Chem. Soc., Chem. Commun*., 1995, 1039.

5 I. G. Dance, *CrystEngComm*, 2003, **5**, 208.

6 (*a*) I. G. Dance and M. L. Scudder, *J. Chem. Soc., Dalton Trans*., 1998, 1341; (*b*) V. Russell, M. L. Scudder and I. G. Dance, *J. Chem. Soc., Dalton Trans*., 2001, 789.

7 M. L. Scudder and I. G. Dance, *Chem.–Eur. J*., 2002, **8**, 5456.

8 T. Steiner, *New J. Chem*., 2000, **24**, 137.

9 (*a*) D. L. Reger, R. F. Semeniuc and M. D. Smith, *Cryst. Growth Des*., 2005, **5**, 1181–1190; (*b*) D. L. Reger, J. R. Gardinier, R. F. Semeniuc and M. D. Smith, *Dalton Trans*., 2003, 1712; (*c*) D. L. Reger, R. F. Semeniuc, J. R. Gardinier, K. J. Brown and M. D. Smith, in *Functional Nanomaterials*, ed. K. E. Geckeler and E. Rosenberg, American Scientific Publishers, Stevenson Ranch, California, 2006, pp. 411–424.

10 (*a*) C. A. Hunter and J. K. M. Sanders, *J. Am. Chem. Soc*., 1990, **112**, 5525; (*b*) C. J. Janiak, *J. Chem. Soc., Dalton Trans*., 2000, 3885 and references therein.

11 (*a*) B. Olenik, R. Boese and R. Sustmann, *Cryst. Growth Des*., 2003, **3**, 175; (*b*) E. V. Garcia-Baez, F. J. Martinez-Martinez, H. Hoepfl and I. I. Padilla-Martinez, *Cryst. Growth Des*., 2003, **3**, 35; (*c*) J. C. Noveron, M. S. Lah, R. E. Del Sesto, A. M. Arif, J. S. Miller and P. J. Stang, *J. Am. Chem. Soc*., 2002, **124**, 6613; (*d*) J. A. Marsden, J. J. Miller, L. D. Shirtcliff and M. M. Haley, *J. Am. Chem. Soc*., 2005, **127**, 2464; (*e*) D. L. Reger, J. D. Elgin, R. F. Semeniuc, P. J. Pellechia and M. D. Smith, *Chem. Commun*., 2005, 4068; (*f*) D. L. Reger, R. F. Semeniuc, J. D. Elgin, V. Rassolov and M. D. Smith, *Cryst. Growth Des*., 2006, **6**, 2758.

12 (*a*) G. R. Desiraju and T. Steiner, *The Weak Hydrogen Bond in Structural Chemistry and Biology*, Oxford University Press, Oxford, 1999; (*b*) G. R. Desiraju, *Chem. Commun*., 2005, 2995; (*c*) P. Metrangolo, H. Neukirch, T. Pilati and G. Resnati, *Acc. Chem. Res*., 2005, **38**, 386; (*d*) C. K. Broder, M. G. Davidson, V. T. Forsyth, J. A. K. Howard, S. Lamb and S. A. Mason, *Cryst. Growth Des*., 2002, **2**, 163; (*e*) L. S. Reddy, S. Basavoju, V. R. Vangala and A. Nangia, *Cryst. Growth Des*., 2006, **6**, 161; (*f*) F. Zordan, L. Brammer and P. Sherwood, *J. Am. Chem. Soc*., 2005, **127**, 5979; (*g*) I. E. D. Vega, P. A. Gale, M. E. Light and S. J. Loeb, *Chem. Commun*., 2005, 4913; (*h*) F. F. Said, T. G. Ong, G. P. A. Yap and D. Richeson, *Cryst. Growth Des*., 2005, **5**, 1881.

13 (*a*) *Design of Organic Solids*, ed. E. Weber, Topics in Current Chemistry, Springer, Berlin, 1998, vol. 198; (*b*) E. Pidcock and W. D. S. Motherwell, *Cryst. Growth Des*., 2005, **5**, 2322; (*c*) M. Du, Z. H. Zhang and X. Zhao, *Cryst. Growth Des*., 2005, **5**, 1199; (*d*) S. Takahashi, T. Katagiri and K. Uneyama, *Chem. Commun*., 2005, 3658; (*e*) R. A. Weatherhead-Kloster, H. D. Selby, W. B. Miller and E. A. Mash, *J. Org. Chem*., 2005, **70**, 8693; (*f*) J. P. Zhang, Y.-Y. Lin, X. C. Huang and X.-M. Chen, *Chem. Commun*., 2005, 1258; (*g*) V. R. Vangala, B. R. Bhogala, A. Dey, G. R. Desiraju, C. K. Broder, P. S. Smith, R. Mondal, J. A. K. Howard and C. C. Wilson, *J. Am. Chem. Soc*., 2003, **125**, 14495; (*h*) A. M. Madalan, V. C. Kravtsov, Y. A. Simonov, V. Voronkova, L. Korobchenko, N. Avarvari and M. Andruh, *Cryst. Growth Des*., 2005, **5**, 45; (*i*) J. N. Moorthy, R. Natarajan, P. Mal and P. Venugopalan, *J. Am. Chem. Soc*., 2002, **124**, 6530.

14 (*a*) S. Iyengar and M. C. Biewer, *Cryst. Growth Des*., 2005, **5**, 2043; (*b*) R. Matsuda, R. Kitaura, S. Kitagawa, Y. Kubota, R. V. Belosludov, T. C. Kobayashi, H. Sakamoto, T. Chiba, M. Takata, Y. Kawazoe and Y. Mita, *Nature*, 2005, **436**, 238; (*c*) K. Kim, K. E. Plass and A. J. Matzger, *Langmuir*, 2005, **21**, 647; (*d*) A. Natarajan, J. T. Mague, K. Venkatesan and V. Ramamurthy, *Org. Lett*., 2005, **7**, 1895; (*e*) S. M. Curtis, N. Le, F. W. Fowler and J. W. Lauher, *Cryst. Growth Des*., 2005, **5**, 2313–2321; (*f*) Y. Morita, T. Murata, K. Fukui, S. Yamada, K. Sato, D. Shiomi, T. Takui, H. Kitagawa, H. Yamochi, G. Saito and K. Nakasuji, *J. Org. Chem*., 2005, **70**, 2739; (*g*) J. L. Atwood, L. J. Barbour and A. Jerga, *Angew. Chem., Int. Ed*., 2004, **43**, 2948; (*h*) K. Sada, K. Inoue, T. Tanaka, A. Tanaka, A. Epergyes, S. Nagahama, A. Matsumoto and M. Miyata, *J. Am. Chem. Soc*., 2004, **126**, 1764; (*i*) K. T. Holman, A. M. Pivovar, J. A. Swift and M. D. Ward, *Acc. Chem. Res*., 2001, **34**, 107; (*j*) N. W. Ockwig, O. Delgado-Friedrichs, M. O'Keeffe and O. M. Yaghi, *Acc. Chem. Res*., 2005, **38**, 176.

15 (*a*) M. Andruh, *Chem. Commun*., 2007, 2565; (*b*) N. R. Champness, *Dalton Trans*., 2006, 877; (*c*) J. D. Wuest, *Chem. Commun*., 2005, 5830; (*d*) K. Biradha, M. Sarkar and L. Rajput, *Chem. Commun*., 2006, 4169; (*e*) Y. Zhou, M. Hong and X. Wu, *Chem. Commun*., 2006, 135.

16 (*a*) A. N. Khlobystov, A. J. Blake, N. R. Champness, D. A. Lemenovskii, G. Majouga, N. V. Zyk and M. Schroder, *Coord. Chem. Rev*., 2001, **222**, 155; (*b*) A. J. Blake, G. Baum, N. R. Champness, S. S. M. Chung, P. A. Cooke, D. Fenske, A. N. Khlobystov, D. A. Lemenovskii, W.-S. Li and M. Schroder, *J. Chem. Soc., Dalton Trans*., 2000, 4285.

17 (*a*) S. T. Batten and R. Robson, *Angew. Chem., Int. Ed*., 1998, **37**, 1460; (*b*) S. Leininger, B. Olenyuk and P. J. Stang, *Chem. Rev*., 2000, **100**, 853; (*c*) G. F. Swiegers and T. J. Malefetse, *Chem. Rev*., 2000, **100**, 3483; (*d*) R. S. Seidel and P. J. Stang, *Acc. Chem. Res*., 2002, **35**, 972; (*e*) L. Carlucci, G. Ciani and D. M. Proserpio, *CrystEngComm*, 2003, **5**, 269; (*f*) Y.-B. Dong, J.-Y. Cheng, R.-Q. Huang, M. D. Smith and H.-C. Zur Loye, *Inorg. Chem*., 2003, **42**, 5699; (*g*) G. B. Gardner, D. Venkataraman, J. S. Moore and S. Lee, *Nature*, 1995, **374**, 792; (*h*) O. M. Yaghi, G. Li and H. Li, *Nature*, 1995, **378**, 703; (*i*) A. J. Blake, N. R. Champness, P. A. Cooke and J. E. B. Nicolson, *Chem. Commun*., 2000, 665; (*j*) A. J. Blake, N. R. Champness, P. A. Cooke and J. E. B. Nicolson Wilson C., *J. Chem. Soc., Dalton Trans*., 2000, 3811; (*k*) R. L. Paul, S. M. Couchman, J. C. Jeffery, J. A. McCleverty, Z. R. Reeves and M. D. Ward, *J. Chem. Soc., Dalton Trans*., 2000, 845; (*l*) M. A. Withersby, A. J. Blake, N. R. Champness, P. Hubberstey, W.-S. Li and M. Schröder, *Angew. Chem., Int. Ed. Engl*., 1997, **36**, 2327.

18 SMART Version 5.625, SAINT+ Version 6.45 and SADABS Version 2.05. Bruker Analytical X-ray Systems, Inc., Madison, Wisconsin, USA, 2001.

19 SHELXTL Version 6.14; Bruker Analytical X-ray Systems, Inc., Madison, Wisconsin, USA, 2000.

20 (*a*) A. Bondi, *J. Phys. Chem*., 1964, **68**, 441; (*b*) R. S. Rowland and R. Taylor, *J. Phys. Chem*., 1996, **100**, 7384.

21 T. Steiner and G. R. Desiraju, *Chem. Commun*., 1998, 891.

22 F. H. Allen, *Acta Crystallogr., Sect. B: Struct. Sci*., 2002, **B58**, 380.

23 I. J. Bruno, J. C. Cole, P. R. Edgington, M. Kessler, C. F. Macrae, P. McCabe, J. Pearson and R. Taylor, *Acta Crystallogr., Sect. B: Struct. Sci*., 2002, **B58**, 389.

24 CCDC (1994). Vista—A Program for the Analysis and Display of Data Retrieved from the CSD; Cambridge Crystallographic Data Centre, 12 Union Road, Cambridge, England.

25 While somewhat arbitrary, the cut-off distance of 7.3 Å was calculated as follows: for simplicity, we considered that one

quinoline moiety overlaps the second having one vertex situated on top of the half C–C distance of the other, as in Scheme 2a. This arrangement makes the distance between the centroid of one quinoline ring to the far vertex of the second ring 5 times the altitude of the equilateral triangle formed by one C–C bond length and the two corresponding centroid-C distances; the cut-off distance of 7.3 Å was found by applying twice the Pythagorean Theorem. Even in such an extreme case, there would still be an overlap of the π cloud of the quinoline rings, as pictured in Scheme 2, with a calculated Ct_2–Ct_4 distance of 4.2 Å.

26 (*a*) A. L. Spek, *J. Appl. Crystallogr*., 2003, **36**, 7; (*b*) PLATON, A Multipurpose Crystallographic Tool, Utrecht University, Utrecht, The Netherlands, Spek, A. L. 2008.
27 L. E. da Silva, A. C. Joussef, S. Foro and B. Schmidt, *Acta Crystallogr., Sect. E: Struct. Rep. Online*, 2006, **62**, m1719.
28 M. R. A. Al-Mandhary and P. J. Steel, *Eur. J. Inorg. Chem*., 2004, 329.
29 G. L. Roberts, B. W. Skelton, A. H. White and S. B. Wild, *Aust. J. Chem*., 1982, **35**, 2193.
30 P. Sangtrirutnugul, M. Stradiotto and T. D. Tilley, *Organometallics*, 2006, **25**, 1607.
31 P. Braunstein, J. Fischer, D. Matt and M. Pfeffer, *J. Am. Chem. Soc*., 1984, **106**, 410.
32 T. Suzuki, *Bull. Chem. Soc. Jpn*., 2004, **77**, 1869.
33 B. Macias, I. Garcia, M. V. Villa, J. Borras, A. Castineiras and F. Z. Sanz, *Z. Anorg. Allg. Chem*., 2003, **629**, 255.
34 A. J. Canty, J. Patel, M. Pfeffer, B. W. Skelton and A. H. White, *Inorg. Chim. Acta*, 2002, **327**, 20.
35 R.-F. Song, Y.-B. Xie, J.-R. Li and X.-H. Bu, *Dalton Trans*., 2003, 4742.
36 S. B. Harkins and J. C. Peters, *Inorg. Chem*., 2006, **45**, 4316.
37 L. M. Engelhardt, G. E. Jacobsen, P. C. Junk, C. L. Raston and A. H. White, *J. Chem. Soc., Chem. Commun*., 1990, 89.
38 T. Ohashi, Y. Miyashita, Y. Yamada, K. Fujisawa and K. Okamoto, *Bull. Chem. Soc. Jpn*., 2003, **76**, 1199.
39 M. Pfeffer, D. Grandjean and G. Le Borgne, *Inorg. Chem*., 1981, **20**, 4426.
40 H. Zhong, X.-R. Zeng, Q.-Y. Luo, M.-L. Li and S.-Z. Xiao, *Acta Crystallogr., Sect. E: Struct. Rep. Online*, 2007, **63**, m492.
41 R.-F. Song, Y.-B. Xie, J.-R. Li and X.-H. Bu, *CrystEngComm*, 2005, **7**, 249.
42 M. C. Kerr, H. S. Preston, H. L. Ammon, J. E. Huheey and J. M. Stewart, *J. Coord. Chem*., 1981, **11**, 111.
43 C.-J. Li, J.-M. Dou, D.-C. Li and D.-Q. Wang, *J. Mol. Struct*., 2006, **784**, 144.
44 J. Andrieu, P. Braunstein, A. Tiripicchio and F. Ugozzoli, *Inorg. Chem*., 1996, **35**, 5975.
45 Y.-H. Wang, R.-F. Song and F.-Y. Zhang, *J. Mol. Struct*., 2005, **752**, 104.
46 J. Kuzelka, J. R. Farrell and S. J. Lippard, *Inorg. Chem*., 2003, **42**, 8652.
47 J. P. Puzas, R. Nakon and J. L. Petersen, *Inorg. Chem*., 1986, **25**, 3837.
48 J. C. Peters, S. B. Harkins, S. D. Brown and M. W. Day, *Inorg. Chem*., 2001, **40**, 5083.
49 J. Taquet, O. Siri, P. Braunstein and R. Welter, *Inorg. Chem*., 2004, **43**, 6944.
50 L. M. Engelhardt, G. E. Jacobsen, P. C. Junk, C. L. Raston, B. W. Skelton and A. H. White, *J. Chem. Soc., Dalton Trans*., 1988, 1011.
51 K. Nehru, S. J. Kim, I. Y. Kim, M. S. Seo, Y. Kim, S.-J. Kim, J. Kim and W. Nam, *Chem. Commun*., 2007, 4623.
52 A. Albinati, F. Lianza, P. S. Pregosin and B. Muller, *Inorg. Chem*., 1994, **33**, 2522.
53 (*a*) H. Takahashi, S. Tsuboyama, Y. Umezawa, K. Honda and M. Nishio, *Tetrahedron*, 2000, **56**, 6185–6191; (*b*) M. Nishio, M. Hirota and Y. Umezawa, *The CH/π Interaction Evidence Nature and Consequences*, Wiley-VCH, New York, 1998; (*c*) S. Tsuzuki, K. Honda, T. Uchimaru, M. Mikami and K. Tanabe, *J. Am. Chem. Soc*., 2000, **122**, 11450–11458.
54 (*a*) T. Steiner, *Angew. Chem., Int. Ed*., 2002, **41**, 48; (*b*) D. Braga, F. Grepioni and E. Tedesco, *Organometallics*, 1998, **17**, 2669.

